Journal of Photochemistry and Photobiology A: Chemistry 205 (2009) 173–178

Contents lists available at ScienceDirect

Journal of Photochemistry and Photobiology A: Chemistry

journal homepage: www.elsevier.com/locate/jphotochem

Improved photocatalytic activity and adsorption ability of mesoporous potassium-intercalated layered titanate

Tae Woo Kim, In Young Kim, Jeong Hyeok Im, Hyung-Wook Ha, Seong-Ju Hwang*

Center for Intelligent Nano-Bio Materials (CINBM), Department of Chemistry and Nano Sciences, College of Natural Sciences, Ewha Womans University, 11-1, Daehyun-dong, Seodaemun-gu, Seoul 120-750, Republic of Korea

ARTICLE INFO

Article history:
Received 18 November 2008
Received in revised form 24 April 2009
Accepted 30 April 2009
Available online 9 May 2009

Keywords:
Exfoliation–reassembling
Mesoporous assembly
Intercalation
Photocatalysis
Adsorption

ABSTRACT

Mesoporous potassium-intercalated layered titanate has been synthesized through a reassembling of exfoliated titanate nanosheets and potassium cations. According to powder X-ray diffraction, electron microscopy, and N_2 adsorption–desorption isotherm analyses, the intercalation of potassium ions gave rise not only to a slight basal expansion of the layered titanate but also to the formation of mesoporous assembly of the layered crystallites. In comparison with the pristine cesium titanate and its protonated derivative, the mesoporous potassium-intercalated titanate showed better photocatalytic activity for the photodegradation of organic molecules and higher adsorption capability for organic dye and CO_2 molecules, as well.

1. Introduction

Over the past decades, mesoporous materials have attracted special interest because of their promising functions as catalysts, adsorbents, gas storing materials, and so on [1–3]. The use of organic surfactants as soft templates proved to be quite useful in synthesizing mesoporous silica-based materials [2]. However, this synthetic strategy is not so effective for the preparation of mesoporous transition metal oxides. This difficulty originates from the unique characteristics of transition metal ions such as rapid hydrolysis, strong preference for high coordination numbers, etc. [2]. On the other hand, the intercalation chemistry of layered transition metal oxide could provide an alternative route to mesoporous transition metal oxide [4–13]. In particular, the exfoliation of layered metal oxide into individually separated nanosheets made it possible to hybrid layered metal oxides with various guest species, leading to new type of porous intercalation compounds [4–9]. Recently we were successful in synthesizing a series of mesoporous hybrid-type transition metal oxides via the intercalative reassembling of 2D metal oxide nanosheets with 0D nanoparticles [4–9]. As a result of electronic coupling between wide bandgap semiconducting titanate and narrow bandgap semiconducting transition metal oxide, visible light active photocatalysts could be produced [4,5,7]. Taking into account the fact that the reassembling between negatively charged titanate nanosheets and positively charged guest species could be achieved in terms of electrostatic interaction, possible guest candidates for the hybridization with the layered titanate are limited to cationic species. In comparison with positively charged metal hydroxide nanoclusters or metal oxide nanoparticles [14], isolated metal cations are expected to be more useful guests for the negatively charged titanate because of their wider pH region for positively charged state. However, there has been no study regarding the intercalative reassembling between layered titanium oxide nanosheets and isolated metal cations.

In this study, we were successful in synthesizing mesoporous potassium-intercalated titanate through the reassembling of exfoliated titanate nanosheets with potassium cations. The crystal structure, crystal morphology, and pore structure of this intercalation compound have been systematically characterized using powder X-ray diffraction (XRD), electron microscopy, and N_2 adsorption–desorption isotherm measurement, respectively. Also, its applicability as environmental photocatalyst and adsorbent for greenhouse gas was investigated by monitoring the photodegradation of methylene blue (MB) under UV–vis irradiation, and the adsorption of CO_2 gas as a function of applied pressure, respectively.

2. Experimental

Layered cesium titanate $Cs_{0.67}Ti_{1.83}\square_{0.17}O_4$ was obtained by solid-state reaction and its protonated derivative was prepared by the subsequent HCl treatment, respectively [4]. The exfoliation of this layered titanate was achieved by reacting the protonated

* Corresponding author. Tel.: +82 2 3277 4370; fax: +82 2 3277 3419.
E-mail address: hwangsju@ewha.ac.kr (S.-J. Hwang).

1010-6030/$ – see front matter © 2009 Elsevier B.V. All rights reserved.
doi:10.1016/j.jphotochem.2009.04.025

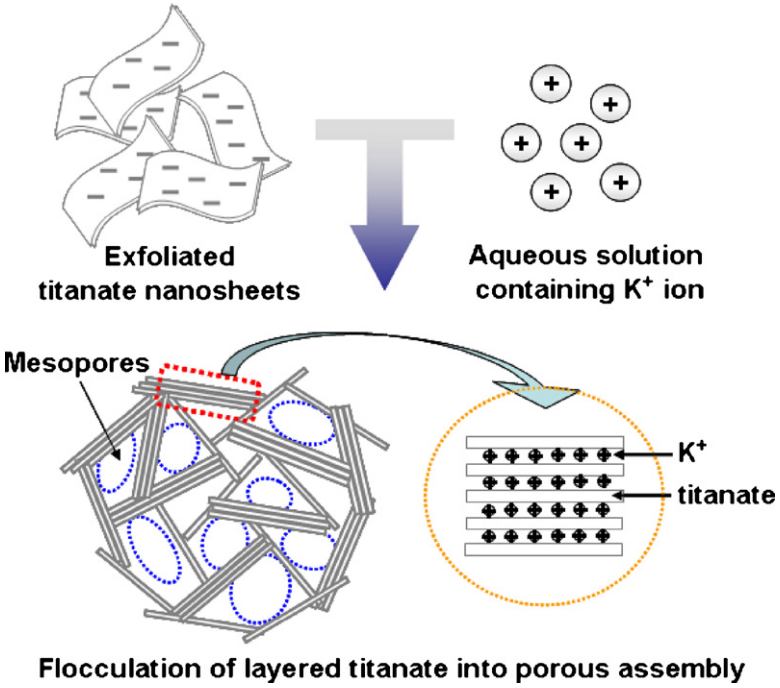

Fig. 1. Schematic model for the reassembling of exfoliated titanate nanosheets and potassium ions.

titanate with tetrabutylammonium hydroxide (TBA·OH) [4]. The reassembling between layered titanate nanosheets and potassium ions was carried out by a dropwise addition of the 5 mL aqueous solution (0.198 mol/L) of potassium hydroxide (0.989 mmol) into the colloidal suspension of exfoliated titanium oxide nanosheets (0.1 g/L, 100 mL) under vigorous stirring. The rate of KOH addition was 0.5 mL/min. The molar ratio of potassium (K) and titanate ($Ti_{1.83}\square_{0.17}O_4$) was adjusted to 15. As illustrated in Fig. 1, the reassembling between both species with opposite charges could be achieved in terms of electrostatic interaction. The resultant products were centrifuged, washed thoroughly with distilled water, and dried in oven. The crystal structure, crystal morphology, chemical composition, and thermal behavior of the potassium-intercalated titanate were studied by powder XRD, field emission-scanning electron microscopy/energy dispersive spectrometry (FE-SEM/EDS, JEOL JSM-6700F microscope), and thermogravimetric analysis (TGA), respectively. The stacking structure of the potassium-intercalates was examined using high resolution-transmission electron microscopy (HR-TEM, Philips-CM200 microscope, 200 kV). The surface area and porosity of this intercalation compound were examined by measuring volumetrically N_2 adsorption–desorption isotherms at liquid nitrogen temperature. The calcined samples were degassed at 150 °C for 2 h under vacuum before the adsorption measurement. Also, the CO_2 adsorption behavior of this material was measured volumetrically at 273.15 K as a function of applied pressure up to 1 atm. Diffuse reflectance UV–vis spectra were obtained on a PerkinElmer Lambda 35 spectrometer equipped with an integrating sphere, using $BaSO_4$ as a reference. The photocatalytic activity of the potassium-intercalated titanate under UV–vis irradiation was examined by adopting MB as a target substrate, in comparison with those of the pristine cesium titanate and its protonated derivative. The substrate was added to an aqueous photocatalyst suspension in the glass reactor (100 mL) with a quartz window and then equilibrated for 30 min with stirring in the dark before illumination. All the tests of photocatalytic reactivity were carried out in aerobic condition. The light from a 400-W Xe arc lamp (Oriel) was passed through a 10-cm IR water filter and a cut-off filter ($\lambda > 300$ nm) and then focused onto the reactor. Sample aliquots were withdrawn intermittently with a 1-mL syringe during the illumination and filtered through a 0.45-μm PTFE filter (Milipore) to remove catalyst particles. The concentration change of MB was monitored spectrophotometrically by measuring the absorbance at $\lambda = 665$ nm with an UV–vis spectrophotometer. Also, the photodegradation of MB was cross-confirmed by monitoring the formation of its decomposition product, i.e. sulfate ion, with ion chromatography (IC).

3. Results and discussions

3.1. Powder XRD analysis

Fig. 2 represents the powder XRD patterns of potassium-intercalated titanate and its calcined derivative, together with those of the pristine cesium titanate, protonated titanate, and exfoliated titanate nanosheets. While the protonated titanate showed a series of well-developed (0*k*0) reflections, no Bragg reflections could be observed for the exfoliated nanosheets of the titanate, indicating the disordered filing of titanate monolayers. After the reaction of the titanate nanosheets with KOH, the (0*k*0) peaks were restored, strongly suggesting the formation of the layer-by-layer ordered intercalation structure. From the least square fitting analysis [15], the basal spacing of the potassium-intercalated titanate was determined to be ~9.15 Å, corresponding to the gallery height of ~1.5 Å. The post-calcination at 200 °C led to a slight displacement of the (0*k*0) reflections toward high angle side, indicating the contraction of basal spacing to ~8.86 Å. This could be interpreted as a result of the removal of interlayer water molecules. In the 2θ range of 22–30°, both the as-prepared and calcined intercalation compounds show a broad and diffuse peak, which originates from the turbostratic/disodered stacking of lamellar titanate nanosheets [16].

3.2. HR-TEM, FE-SEM, and chemical analyses

The formation of intercalation structure upon the reaction between KOH and titanate nanosheets was confirmed by HR-TEM

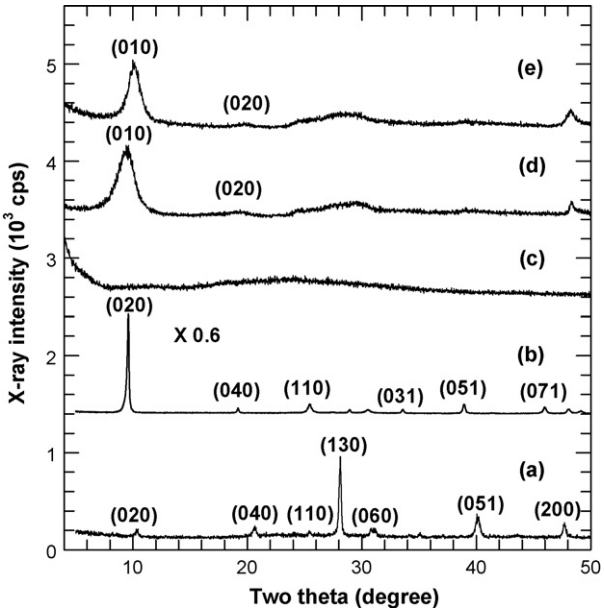

Fig. 2. Powder XRD patterns of (a) cesium titanate, (b) protonated titanate, (c) the colloidal particles of exfoliated titanate, (d) potassium-intercalated titanate and (e) its derivative calcined at 200 °C.

analysis. As shown in Fig. 3, the exfoliated titanate nanosheets are reassembled in layer-by-layer way during the intercalation of potassium ions into layered titanate. The cross-sectional HR-TEM image of the potassium-intercalated titanate clearly demonstrated its interstratification structure with the basal spacing of ~0.91 nm.

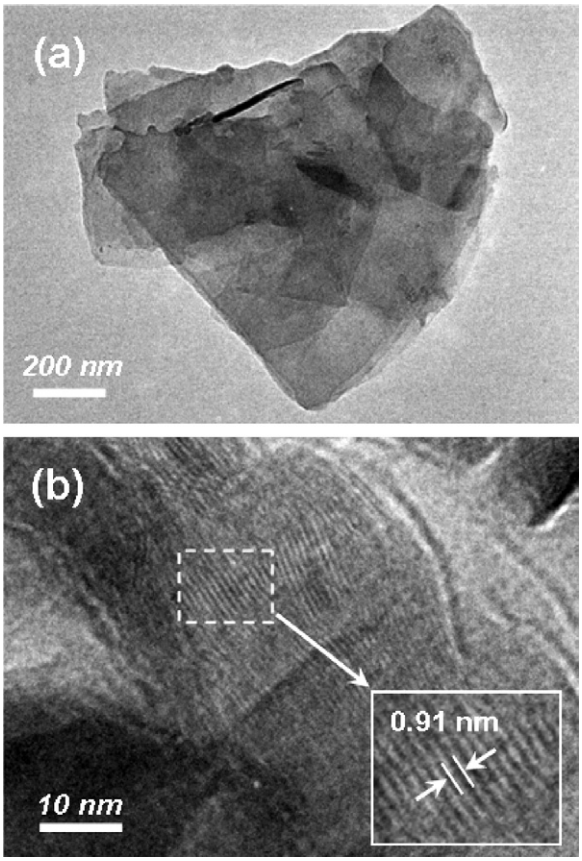

Fig. 3. HR-TEM images of the potassium-intercalated layered titanate; (a) top view and (b) cross-sectional view.

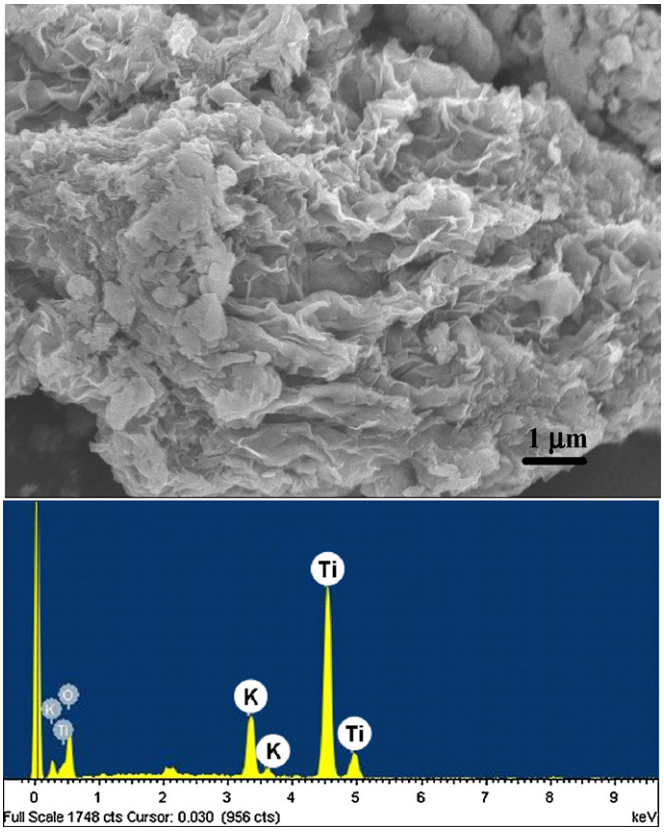

Fig. 4. (Top) FE-SEM image and (bottom) EDS graph of the potassium-intercalated layered titanate calcined at 200 °C.

The estimated basal spacing is in good agreement with the value obtained from powder XRD analysis (Fig. 2).

Also, we have examined the crystal morphology and cation composition of the present intercalation compound using FE-SEM/EDS tool. As illustrated in Fig. 4, the layered crystallites of the intercalation compound are stacked to form house-of-cards type porous assembly, suggesting the formation of mesopores upon the reassembling reaction. On the other hand, we have determined the cation composition of the potassium-intercalated titanate from the relative intensity of the EDS peaks. As shown in Fig. 4, the ratio of K/Ti was estimated to be 0.29, which is slightly lower than the Cs/Ti ratio in the pristine cesium titanate (0.37). The observed discrepancy in cation composition would reflect the presence of small amount of protons in the potassium-intercalated titanate to compensate the excess negative charge of the titanate layers. On the other hand, we have examined the thermal behavior of the potassium-intercalated titanate using TGA. As plotted in Fig. 5, the present intercalation compound exhibits marked weight losses to 150 °C, which corresponds to the evaporation of water molecules. From the amount of weight decrease and EDS results, the chemical formula of the as-prepared intercalate was determined to be $K_{0.53}H_{0.14}Ti_{1.83}\square_{0.17}O_4{\cdot}0.83H_2O$.

3.3. Gas adsorption and UV–vis spectroscopic analyses

As found from the TGA results presented here (Fig. 5), the intercalation compound prepared in aqueous media contains significant amount of water molecules adsorbed on the surface and/or in the pores [17]. Such water molecules would block the adsorption of gas molecules onto the intercalation compound. In this regard, we have measured the porosity of the intercalation compound after removing the adsorbed water molecules by the calcination at 200 °C. The

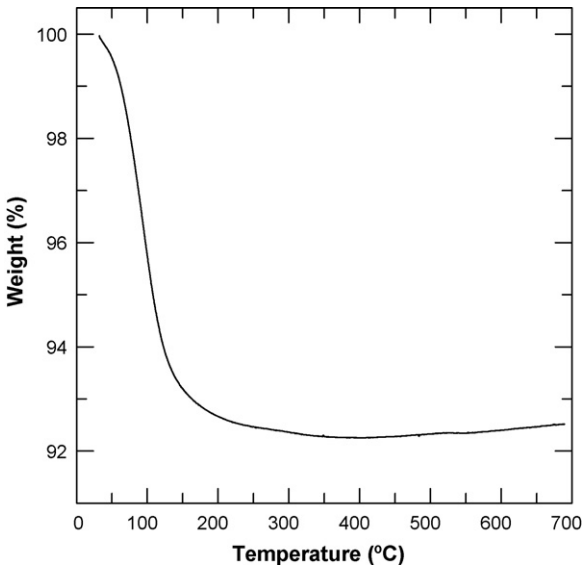

Fig. 5. TGA curve of the potassium-intercalated layered titanate.

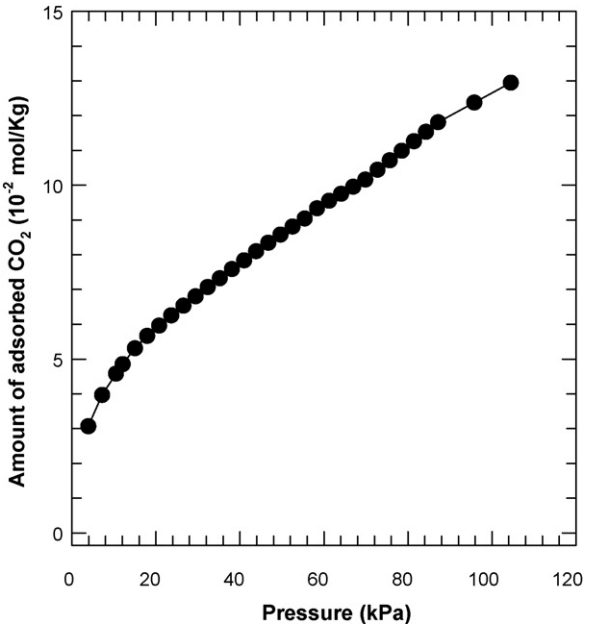

Fig. 7. CO_2 adsorption behavior of potassium-intercalated titanate calcined at 200 °C at 273.15 K.

N_2 adsorption–desorption isotherm of the potassium-intercalated titanate is plotted in Fig. 6. A distinct hysteresis appeared in the pressure region of $p/p_0 > 0.4$, indicating the formation of mesoporous structure originating from the house-of-cards stacking of the layered crystallites. The observed hysteresis behavior could be classified as the Brunauer–Deming–Deming–Teller (BDDT) type I and IV shape, along with H3-type hysteresis loop in the IUPAC classification [18]. This indicates the presence of the open slit-shaped capillaries with very wide bodies and narrow short necks. The surface area of this intercalation compound (~8 m^2/g) was determined to be larger than that of the pristine titanate (~1 m^2/g), highlighting the increase of surface area after the intercalation. To estimate the pore size of the obtained intercalation compound, we have analyzed its pore distribution with Barrett–Joyner–Halenda (BJH) method. As plotted in the inset of Fig. 6, the pores in this intercalation compound possess a quite narrow size distribution with an average pore diameter of ~5.2 nm. This pore size could be reproducibly obtained under the synthetic condition given in the experimental section. Taking into account the fact that the obtained pore size is much larger than the basal spacing of the intercalation structure, the formation of this mesopore is surely attributable to the disordered porous stacking of the potassium–titanate crystallites, as suggested from the FE-SEM result. In fact, we have found that, regardless of the types of guest species, the reassembling process of exfoliated titanate nanosheets creates mesopores with the similar size of ~5 nm [4,5]. We have tested the capability of this intercalation compound for the adsorption of greenhouse gas like CO_2. As shown in Fig. 7, the potassium-intercalated titanate could induce a distinct adsorption of CO_2 gas molecules at 273.15 K. Even though the amount of CO_2 gas adsorbed is somewhat small, the present result suggests that, after the optimization of the surface area, the obtained titanate-based intercalation compound can be used as adsorbent for gaseous carbon dioxide.

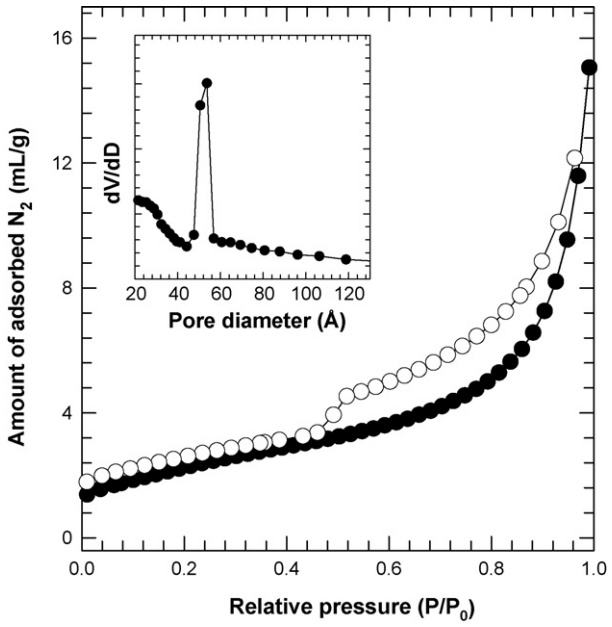

Fig. 6. N_2 adsorption–desorption isotherm and (inset) pore size distribution curve analyzed by BJH method for the potassium-intercalated layered titanate calcined at 200 °C.

On the other hand, evolution of the band structure of layered titanate upon potassium intercalation has been investigated with diffuse reflectance UV–vis spectroscopy. As shown in Fig. 8, a clear absorption edge commonly appeared beyond 3.5 eV for the pristine cesium titanate and, its protonated and potassium-intercalated derivatives, highlighting the wide bandgap semiconducting nature of these materials. From an interpolation process, the bandgap energy of the potassium-intercalated titanate was determined to be ~3.5 eV, which is almost identical to those of the pristine titanate and its protonated derivative. Little change of the bandgap energy of titanate upon the potassium intercalation is attributed to the inactivity of potassium ion to UV–vis absorption.

3.4. Photocatalyst test

The photocatalytic activity of the potassium-intercalated titanate was tested against the photodegradation of MB in an illuminated catalyst suspension, in comparison with those of the pristine cesium titanate and its protonated derivative. In order to separate the effect of adsorption of organic molecule, we have soaked the photocatalyst in substrate solution for 30 min in dark condition. Of special interest is that large amount of the MB dye molecules (~80%) could be adsorbed by the potassium-intercalated compound in the

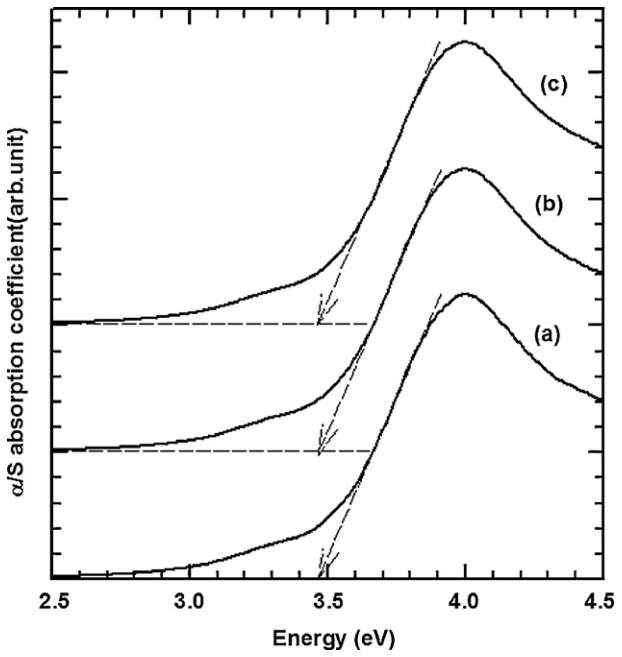

Fig. 8. Diffuse reflectance UV–vis spectra of (a) cesium titanate, (b) protonated titanate, and (c) potassium-intercalated titanate.

dark. This result contrasted well with negligible MB adsorption by the cesium titanate and the protonated titanate, underscoring the remarkable enhancement of the adsorption capability of the layered titanate upon the potassium intercalation. It is worthwhile to mention that the effective adsorption of pollutant molecules by porous solids is important for the rapid purification of contaminated water. We have monitored the photodegradation of MB molecules under UV–vis irradiation ($\lambda > 300$ nm) by measuring the UV–vis spectra of supernant solution. As displayed in Fig. 9, both the cesium titanate and protonated titanate appeared inactive for the photodegradation of MB molecules, whereas the potassium-intercalate led to notable decrease of the dye concentration. The photodegradation of MB molecules by the potassium-intercalated

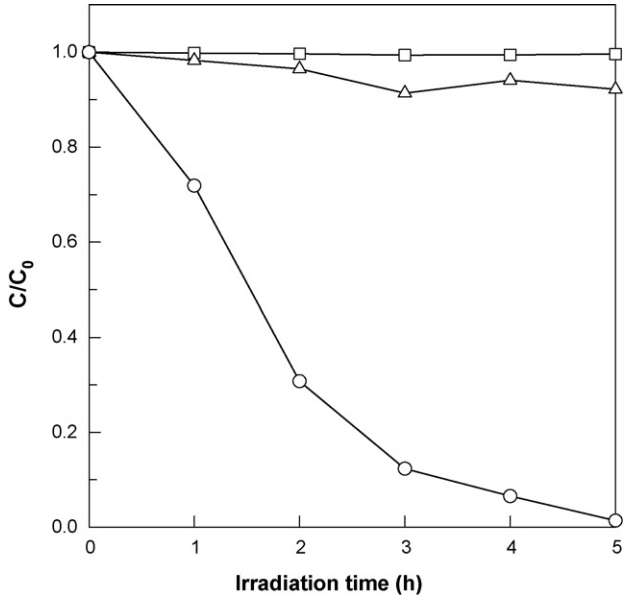

Fig. 9. Time profiles of photocatalytic degradation of MB in UV–vis illuminated ($\lambda > 300$ nm) suspensions of the potassium-intercalated titanate calcined at 200 °C (○) and the pristine cesium titanate (△) and protonated titanate (□).

titanate was cross-confirmed by the IC analysis for the supernant solution revealing the formation of sulfate ion, i.e., a decomposition product of MB molecule. Summarizing all the findings presented here, it becomes certain that the formation of porous structure by the potassium intercalation markedly improves the photocatalytic activity of the layered titanate. Considering negligible change of bandgap energy upon the potassium intercalation, the observed increase of photocatalytic activity can be attributed to the increase of surface area by the formation of porous structure [19]. The expansion of surface area implies the provision of larger number of reaction sites on the catalyst surface, leading to the improvement of the photocatalytic activity.

4. Conclusions

In this work, we have successfully synthesized mesoporous potassium-intercalated layered titanate. The formation of potassium intercalation compound was confirmed by powder XRD and HR-TEM/FE-SEM analyses. N_2 adsorption–desorption isotherm measurements with BJH pore analyses clearly demonstrated that the present intercalation compound possesses mesopores with a narrow size distribution (average diameter ~5.2 nm). Also, we have found that the present mesoporous intercalation compound shows better photocatalytic activity for the photodegradation of organic molecules and higher adsorption capability for organic dye and CO_2 molecules, indicating its applicability as environmental photocatalyst and absorbent for greenhouse gas. On the basis of the present experimental findings, it became clear that the reassembling reaction between exfoliated titanate nanosheets and metal ions is useful for synthesizing new type of mesoporous materials with multiple functions.

Acknowledgment

This work is the outcome of a Manpower Development Program for Energy & Resources supported by the Ministry of Knowledge and Economy (MKE) and partly supported by the SRC/ERC program of the MOST/KOSEF (grant: R11-2005-008-03002-0).

References

[1] A. Corma, From microporous to mesoporous molecular sieve materials and their use in catalysis, Chem. Rev. 97 (1997) 2373–2420, and the references therein.
[2] G.J. De, A.A. Soler-Illia, C. Sanchez, B. Lebeau, J. Patarin, Chemical strategies to design textured materials: from microporous and mesoporous oxides to nanonetworks and hierarchical structures, Chem. Rev. 102 (2002) 4093–4138, and the references therein.
[3] D.E. De Vos, M. Dams, B.F. Sels, P.A. Jacobs, Ordered mesoporous and microporous molecular sieves functionalized with transition metal complexes as catalysts for selective organic transformations, Chem. Rev. 102 (2002) 3615–3640.
[4] T.W. Kim, S.-J. Hwang, S.H. Jhung, J.-S. Chang, H. Park, W. Choi, J.-H. Choy, Bifunctional heterogeneous catalysts for selective epoxidation and visible light driven photolysis: nickel oxide-containing porous nanocomposite, Adv. Mater. 20 (2008) 539–542.
[5] T.W. Kim, S.G. Hur, S.-J. Hwang, H. Park, W. Choi, J.-H. Choy, Heterostructured visible-light-active photocatalyst of chromia-nanoparticle-layered titanate, Adv. Funct. Mater. 17 (2007) 307–314.
[6] T.W. Kim, S.G. Hur, S.-J. Hwang, J.-H. Choy, Layered titanate–zinc oxide nanohybrids with mesoporosity, Chem. Commum. (2006) 220–222.
[7] T.W. Kim, S.-J. Hwang, Y. Park, W. Choi, J.-H. Choy, Chemical bonding character and physicochemical properties of mesoporous zinc oxide-layered titanate nanocomposites, J. Phys. Chem. C 111 (2007) 1658–1664.
[8] T.W. Kim, A.R. Han, S.-J. Hwang, J.-H. Choy, Local atomic arrangement and electronic configuration of nanocrystalline zinc oxide hybridized with redoxable 2D lattice of manganese oxide, J. Phys. Chem. C 111 (2007) 16774–16780.
[9] T.W. Kim, H.-W. Ha, M.-J. Paek, S.-H. Hyun, J.-H. Choy, S.-J. Hwang, Mesoporous iron oxide-layered titanate nanohybrids: soft-chemical synthesis, characterization, and photocatalyst application, J. Phys. Chem. C 112 (2008) 14853–14862.
[10] S.G. Hur, T.W. Kim, S.-J. Hwang, S.H. Hwang, J.H. Yang, J.-H. Choy, Heterostructured nanohybrid of zinc oxide-montmorillonite clay, J. Phys. Chem. B 110 (2006) 1599–1604.

[11] J.H. Park, J.H. Yang, J.B. Yoon, S.-J. Hwang, J.-H. Choy, Intracrystalline structure and physicochemical properties of mixed SiO_2–TiO_2 sol-pillared aluminosilicate, J. Phys. Chem. B 110 (2006) 1592–1598.
[12] S.M. Paek, H. Jung, Y.J. Lee, M. Park, S.-J. Hwang, J.-H. Choy, Exfoliation and reassembling route to mesoporous titania nanohybrids, Chem. Mater. 18 (2006) 1134–1140.
[13] H.M. Park, T.W. Kim, S.-J. Hwang, J.-H. Choy, Chemical bonding nature and mesoporous structure of nickel intercalated montmorillonite clay, Bull. Kor. Chem. Soc. 27 (2006) 1323–1328.
[14] C.F. Baes Jr., R.E. Mesmer, The Hydrolysis of Cations, John Wiley & Sons, New York, 1982.
[15] Since there are two titanate layers in the unit cell of the pristine cesium titanate and the protonated titanate, the d_{020} value of both compounds corresponds to the sum of gallery height and layer thickness, like the d_{010} value of the intercalation compound.
[16] T. Sasaki, S. Nakano, S. Yamauchi, M. Watanabe, Fabrication of titanium dioxide thin flakes and their porous aggregate, Chem. Mater. 9 (1997) 602.
[17] M.S. Dresselhaus, Intercalation in Layered Materials, Plenum Press, New York, 1986.
[18] S.J. Gregg, K.S.W. Sing, Adsorption, Surface Area and Porosity, Academic Press, London, 1976.
[19] M.R. Hoffmann, S.T. Martin, W. Choi, D.W. Bahnemann, Environmental applications of semiconductor photocatalysis, Chem. Rev. 95 (1995) 69–96.